

UNCLASSIFIED

AD 417190

DEFENSE DOCUMENTATION CENTER

FOR

SCIENTIFIC AND TECHNICAL INFORMATION

CAMERON STATION, ALEXANDRIA, VIRGINIA



UNCLASSIFIED

NOTICE: When government or other drawings, specifications or other data are used for any purpose other than in connection with a definitely related government procurement operation, the U. S. Government thereby incurs no responsibility, nor any obligation whatsoever; and the fact that the Government may have formulated, furnished, or in any way supplied the said drawings, specifications, or other data is not to be regarded by implication or otherwise as in any manner licensing the holder or any other person or corporation, or conveying any rights or permission to manufacture, use or sell any patented invention that may in any way be related thereto.

May 1-7  
D1-82-0244

CATALOG  
AS

*Also available from the author*

# BOEING SCIENTIFIC RESEARCH LABORATORIES

Power Spectral Density Estimates  
of the Fading of High Frequency  
Radio Waves

D. H. Schrader

May 1963

Geo-Astrophysics Laboratory

(1)

DL-80-0744

POWER SPECTRAL DENSITY ESTIMATES OF THE FADING  
OF HIGH FREQUENCY RADIO WAVES

by

D. H. Schrader

Geo-Astrophysics Laboratory

Boeing Scientific Research Laboratories

Seattle 24, Washington

and

Electrical Engineering Department

University of Washington

Seattle, Washington

May 1963

## ABSTRACT

The power spectral density of the fading power of high-frequency radio waves and methods of estimating this function are the subject of this report.

Evaluations of the power spectral density estimates obtained by two different methods are made. The asymptotic low-frequency variation of estimates computed on a digital computer and the expected value of estimates computed with an analog computer are derived. A comparison of the two methods is made and power spectral density estimates computed by both methods are shown.

Power spectral density estimates are shown for eight different data samples. In general, the power density is confined to frequencies below one cycle per second.

---

#### ACKNOWLEDGMENTS

The author wishes to express appreciation to the Boeing Scientific Research Laboratories and to thank Professor H. M. Swarm of the University of Washington for his direction of this research. He also wishes to acknowledge the cooperation and use of the facilities of the analog computer and the Radio Propagation Laboratories of the Electrical Engineering Department at the University of Washington.

---

## TABLE OF CONTENTS

	Page
1. INTRODUCTION	1
2. NATURE OF THE RECORDS	2
3. DESCRIPTION OF THE IONOSPHERIC PHENOMENA	3
4. MATHEMATICAL MODELS	9
5. DIGITAL COMPUTER PROGRAM	12
6. STATISTICAL TEST OF THE SPECTRAL ESTIMATES	14
7. STATISTICAL PROPERTIES OF THE SPECTRAL ESTIMATES	20
8. ANALOG COMPUTER PROGRAM	31
9. EXPECTED VALUE OF THE SPECTRAL ESTIMATES	37
10. RESULTS	44
11. CONCLUSIONS	59
APPENDIX A - Equipment	60
REFERENCES	63

LIST OF FIGURES

	Page
Fig. 1. Detected 17.9 mc signal from 1422 to 1433 PST on August 4, 1960. The propagation path length is 6,000 km. Signal strength increases downward.	4
Fig. 2. Detected WWV (20 mc) signal from 2349 GMT on May 9, 1962 to 0045 GMT on May 10, 1962. The propagation path is 3710 km. Signal strength increases upward.	5
Fig. 3. Auto-correlation function of the detected 17.9 mc signal from 1431:18 to 1436:20 PST, August 4, 1960.	25
Fig. 4. Auto-correlation function of the detected 11.9 mc signal from 1616:09 to 1618 PST, June 15, 1960.	26
Fig. 5. Analog computer circuit.	32
Fig. 6. Analog computer output voltages.	34
Fig. 7. Weighting function in $E [S_e(\omega)]$ .	43
Fig. 8. Power spectral density estimate of the fading power in the detected 17.9 mc signal, August 4, 1960, as computed by digital and analog methods.	47
Fig. 9. Power spectral density estimate of the fading power in the detected 11.9 mc signal from 1616:09 to 1618 PST, June 15, 1960.	48

	Page
Fig. 10. Power spectral density estimate for the 15.1 mc signal power level fluctuations from 1830:40 to 1848:40 PST on July 31, 1960.	51
Fig. 11. Power spectral density estimate for the 17.9 mc signal power level fluctuations from 1404 to 1417:30 PST on August 4, 1960.	52
Fig. 12. Power Spectral density estimate for the 17.9 mc signal power level fluctuations from 1421 to 1443 PST on August 4, 1960.	53
Fig. 13. Power spectral density estimate for the 15.1 mc signal power level fluctuations from 1644 to 1658 PST on September 22, 1960.	54
Fig. 14. Power spectral density estimate for the 20 mc WWV signal power level fluctuations from 2249 to 2345 GMT on May 9, 1962.	55
Fig. 15. Power spectral density estimate for the 20 mc WWV signal power level fluctuations from 2349 GMT on May 9, 1962 to 0045 GMT on May 10, 1962.	56

## 1. Introduction

The purpose of this investigation was to make a study of the statistical character of fading radio waves. In particular the power spectral density of the amplitude of the fading waves was studied. Several samples of data were statistically analyzed in order to obtain estimates of the true power density spectrum of the underlying random process. The estimates were computed in two different ways: the first way utilized a digital computer and the second an analog computer.

A theoretical evaluation of the methods of computing the estimates of the power density spectrum was also undertaken in order to aid the interpretation of the estimates. The expected value of the estimates that were calculated with the aid of an analog computer was derived and the nature of the variation of the expected value of the digitally computed estimates was ascertained. A comparison of the digital method with the analog method was made.

The next two sections of the report deal with the nature of the data and the ionosphere. The fourth section discusses the statistical models characterizing the observed process. The next three sections describe the digital computer program for obtaining estimates of the power spectral

density, statistical tests of these estimates and the asymptotic variation of the expected value of these estimates for low frequencies. The last part of Section 7 contains a comparison of the digital computer method and the analog computer method of estimating the spectrum. The next two sections describe the analog computer method and a derivation of the expected value of the power spectral density estimates obtained with this method. The last two sections present the results and conclusions of the study.

## 2. Nature of the Records

The records of the amplitude of the fading radio waves were obtained by recording on magnetic tape the detected voltage out of the IF strip of a receiver. The receiver was adjusted so that the output was directly proportional to the radio-frequency input over the operating range.

For some of the data the signals received by the receiver had been transmitted over a 6000 km path and most probably were reflected three or four times by the ionosphere. Signal frequencies of 11.9, 15.1 and 17.9 Mc were used. These signals were cw, keyed for identification every half of an hour. The remainder of the data

consists of recordings of the amplitude of WWV at 20 mc.

Examination of data samples (Figures 1 and 2) shows that the signal underwent considerable variation but that the variation was not rapid, usually requiring more than one fifth of a second for any considerable change in magnitude.

### 3. Description of the Ionospheric Phenomena

The mathematics describing the statistics of the amplitude of the reflected radio wave should be based upon some physical model. The physical model envisioned in most attempts to explain the fading phenomenon is an ionized medium which does not have a uniform ionization density throughout its extent. This medium is called the ionosphere. Due to the non-uniform ionization some regions of the ionosphere will reflect radiation more effectively than other regions. These regions of ionization are continually forming and dissipating and are moving with different velocities. The motion of these regions causes radio waves to suffer a Doppler frequency shift. The radio wave that is finally received from this scattering process then is a wave which might be thought of as being composed of components differing slightly in frequency and differing in propagation path, which combine in such a way as to yield a wave varying in amplitude and in phase.

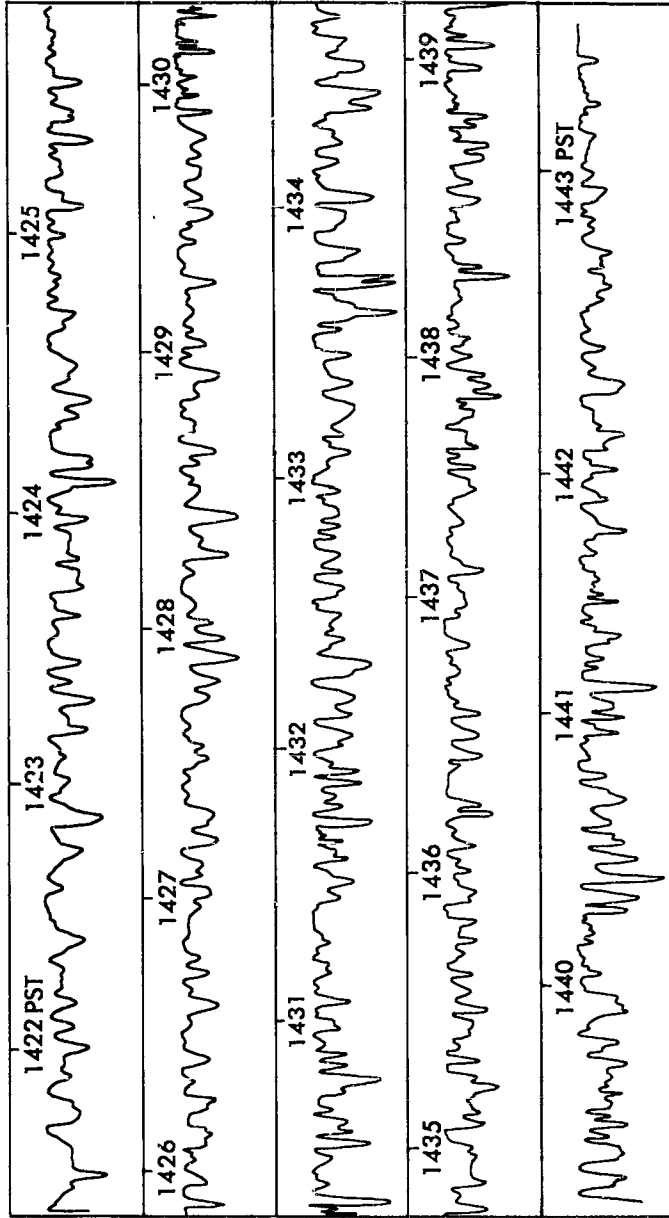


Fig. 1. Detected 17.9 mc signal from 1422 to 1443 PST on August 4, 1960. The propagation path length is 6,000 km. Signal strength increases downward.

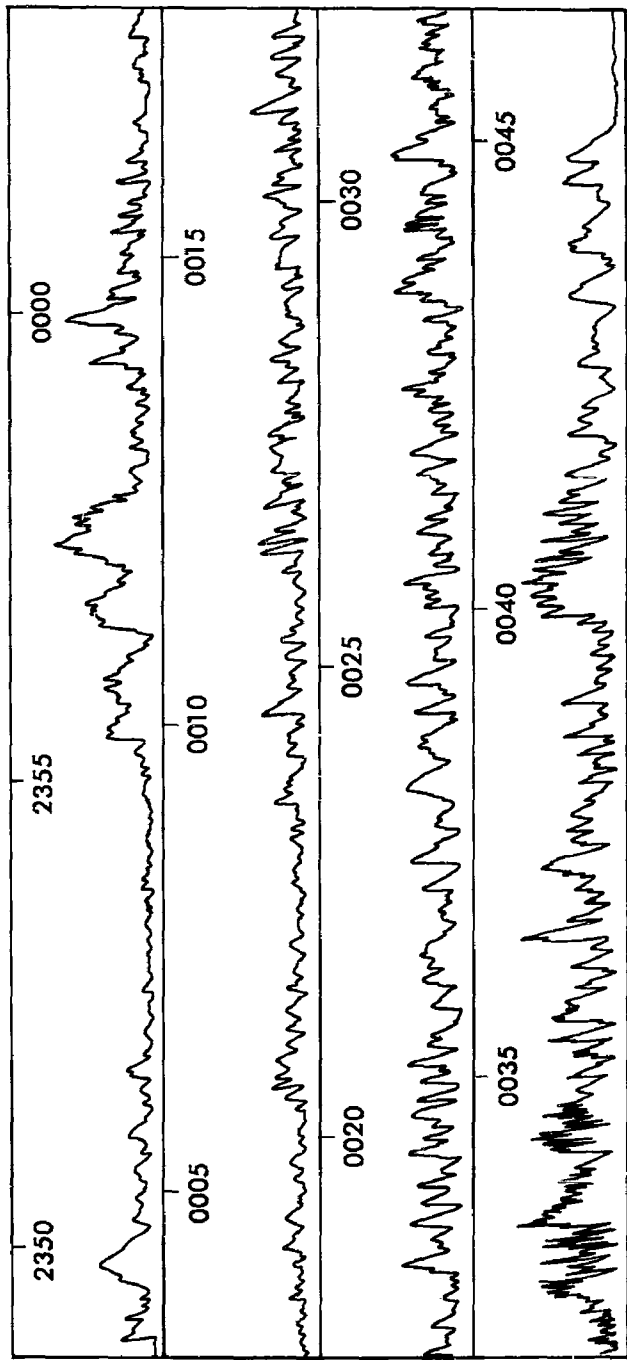


Fig. 2. Detected WWV (20 mc) signal from 2349 GMT on

May 9, 1962 to 0045 GMT on May 10, 1962. The

propagation path is 3710 km. Signal strength

increases upward.

The treatment of the problem depends upon several parameters. These are (a) the size of the scattering regions ('spots') in the ionosphere, (b) the number per unit volume, (c) the rate of formation and disappearance of these regions, (d) the average velocity of these spots and (e) the uniformity of motion of these spots.

Whether many or few scattering regions in the ionosphere are actively contributing to the signal reception at any given time is unknown. During sunrise or sunset periods Yeh and Villard <sup>(1)</sup> have noticed a sinuous type of fading which they attribute to the simultaneous reception of the signal via two distinct modes of propagation. It has been speculated that one of the modes of propagation is caused by an ionospheric tilt which moves westward with the sun. The motion of the tilt imparts a relatively large Doppler frequency shift to one of the received waves. The other wave is supposed to be due to ordinary reflection by the ionosphere. The two waves then combine to produce a single wave which has a sinuous type of modulation. This effect also has been noticed by Nicholson. <sup>(2)</sup>

Pertinent to the subject of fading of reflected waves is the information gained by Wild and Roberts <sup>(3)</sup> when studying the variations of amplitude of extra-terrestrial

noise that had been received after passing through the ionosphere. In this case the ionosphere is assumed to act as a diffracting screen which is continually changing its structure as well as moving around. These experimenters recorded the amplitude of the received signal versus time and frequency, using a radio star in the constellation of Cygnus as the source of radiation. The receiver was swept over the frequency range of 40 to 70 mc. The period of time required to sweep the receiver was short with respect to the time required for changes in amplitude of the received signal at any given frequency in the range.

From these measurements they were able to determine that the amplitude fading appeared to be created, at least some of the time, by a single diffracting irregularity of large dimension which was moving past the receiver. The difference between the conditions of this test and the conditions of an experiment measuring the fading of a reflected signal are many. In the first place the area of the ionosphere involved in the experiment is probably smaller for the diffraction type of experiment than for the reflection type of experiment. Secondly, there is the possibility of several modes of propagation existing simultaneously in the normal HF radio link. However, some results that are useful in describing the fading of

reflected waves have been obtained in the diffraction type of experiment.

The motion of the ionosphere has been investigated by a number of researchers. Briggs and Spencer <sup>(4)</sup> have mentioned speeds on the order of 80 meters per second, using the method of spaced receivers which was developed by S. N. Mitra. <sup>(5)</sup> There is some doubt as to the accuracy of these figures because of the assumptions inherent in the method concerning the shape of the irregularities. Motions measured by reflection from meteor trails establish speeds on the order of 70 meters per second according to Manning and Eshleman. <sup>(6)</sup> Measurements of sodium vapor clouds indicate horizontal wind velocities of 140 meters per second. <sup>(7)</sup> Velocities reported by Wild and Roberts derived from radio-star scintillation measurements are 20 meters per second after removal of apparent motion due to rotation of the earth. <sup>(3)</sup>

The time of growth and decay of small scale (30 km) irregularities as measured by a backscatter experiment has been reported by Barry <sup>(8)</sup> to be ten minutes on the average.

Spencer <sup>(9)</sup> indicates that irregularities measured by virtue of their diffraction of extra-terrestrial waves at 38 mc were elongated by a factor of at least 5:1 possibly along the direction of the geomagnetic field lines.

The motion of the ionosphere appears to be, in the large sense, a uniform motion of the whole reflecting portion of the ionosphere. However, Court <sup>(10)</sup> reports that there is some randomness in the varying radio waves that cannot be explained on the basis of a uniformly translating ionosphere.

These results seem to suggest that only a small number of scatterers is usually effective in causing the amplitude of reflected waves to vary. The scale of turbulence seems to suggest that at least part of the fading is caused by an interference pattern moving past the receiver that is due to the scattering from a large region of the ionosphere moving through the illuminated area of the ionosphere.

#### 4. Mathematical Models

In considering mathematical models which might possibly describe in a statistical sense the varying amplitude of the received wave we might consider the wave received at the receiver as a discrete sum of received signals, each signal being thought of as having been scattered from a particular spot whose dimensions are all smaller than a wavelength. In this case the randomness of the variation of the amplitude of the received signal would arise from variations in (a) the number of such point scatterers inside the intersection of

the transmitting and receiving antenna cones, (b) the strength of the scattered signal from each of the scatterers, (c) the component of velocity of each spot in the direction of transmission, and (d) the instantaneous phase angle of the return from the individual spot.

Another possible way of viewing this problem is to consider a Markov chain in which states of the chain are constructed from the possible diffraction patterns associated with scattering from irregularities which have dimensions on the order of many wavelengths. The states would be defined by the existence of any one of these patterns or of combinations of these patterns. A factor which must enter into the delineation of the states is the speed with which the diffraction patterns are moving past the receiver. This type of Markov chain is too complex to handle in a simple fashion.

If we may assume that the process is stationary we can learn something from the power spectral density of the amplitude records. If there is no power density above say 10 cycles per second one might intuitively expect the ionosphere to be relatively constant in a period of 1/10 of a second. If the power density were spread uniformly over a wide range of frequencies one might expect the signal was composed of many random components. If there were two signals adding

to form the received signal such that one of these component signals had suffered a Doppler frequency shift one might expect a large amount of fading power in a small region of frequency about the value of the Doppler frequency shift.

As shown later, power spectral density estimates made from fade records fluctuate wildly as functions of frequency. The ratio of a maximum value to the adjacent minimum value may be as high as three for a typical record. One wonders whether these peaks in the spectral estimates are indicative of randomly occurring periodicities in the fade records or whether these fluctuations normally occur as deviations of the estimates from the true value of the spectrum. This question is inextricably related to the question of whether adjacent (in time) data points are statistically independent samples.

The sample theorem tells us that when the true power spectral density function is essentially zero above some frequency,  $f_u$ , the time period between samples need not be less than  $2/f_u$ . However, samples taken this close together are obviously not independent samples but are very well correlated. On the other hand, if we take samples separated by a time period  $\Delta t$  which is much larger than  $2/f_u$  so that the samples are independent then we can derive no information

concerning the shape of the spectrum between the frequency  $f = 1/(2\Delta t)$  and the frequency  $f_u$ .

When the sample points are well correlated the task of finding the expected value and the standard deviation of the spectral estimates (i.e., the task of deciding how greatly the spectral estimates might vary from the true spectrum) becomes difficult.

Despite these difficulties the time increment between sample points was chosen small enough so that no extreme amplitude change occurred between samples.

#### 5. Digital Computer Program

The problem of estimating the power spectral density of the process from the amplitude records was handled in two different ways. One method was to simulate a low frequency spectrograph of adjustable Q with an analog computer. The other method involved using the digital computer and discrete data points to estimate the auto-correlation function and then, from this function, to estimate the power spectral density.

The second method mentioned was used to obtain only a few estimates of the power spectral density. The program for obtaining these estimates is described in a Boeing

report. (11) The estimates of the auto-correlation function,  $R(m)$ , were computed by using the formula

$$R(m) = \frac{1}{N-m} \sum_{n=1}^{N-m} H(n\Delta t) H[(n+m)\Delta t], \text{ for } m = 0, 1, 2, \dots, [N/4], \quad 5.1$$

where  $[H(n\Delta t)]^{1/2}$  is equal to the difference between the data (as a function of time) and the average value of the data, and where  $N$  is the total number of data points. The estimates of the power spectral density  $S_e(2\pi k\Delta g)$  were then computed by the use of the formula

$$S_e(2\pi k\Delta g) = 4\Delta t \left[ \frac{R(0)}{2} + \sum_{m=1}^{[N/4]} R(m) \cos(2\pi k\Delta g m\Delta t) \right], \quad 5.2$$

where  $k$  is an integer and  $\Delta g$  is the increment of frequency. The subscript  $e$  denotes the estimated value of  $S$ . These formulas are approximations to the formulas

$$R(\tau) = 1/T \int_{-T/2}^{T/2} f_1(t) f_1(t + \tau) dt \quad 5.3$$

and

$$S(\omega) = 4 \int_0^{T/4} R(\tau) \cos(\omega\tau) d\tau. \quad 5.4$$

No weighting function was used in the calculation of the auto-correlation estimate (i.e., in the terminology of Blackman and Tukey <sup>(12)</sup>, the 'lag window' was a square window); hence, power density at a discrete frequency will appear in the estimate as a  $(\sin u)/u$  function centered about the frequency of the power density.

The digital computer program did not turn out to be as useful as had been anticipated since the amount of computer time required to handle reasonably long data samples was much too great.

#### 6. Statistical Test of the Spectral Estimates

Under certain conditions one may derive some quantitative information concerning the true power spectral density from the spectral estimates using a statistical test of the magnitude of the estimate. That is, if the random process, of which the data constitute a sample function, is a stationary, ergodic, random process and if the original process is a Gaussian process, then a probability distribution defined over the amplitude of the power spectral density estimate may be calculated. From this probability distribution one may find the probability of obtaining any given value when computing the power spectral density estimate. If the spectral estimate obtained has a small probability one

makes the inference that either the conditions of stationarity and ergodicity or the requirement that the process be a Gaussian process did not hold.

The test described above is modified from a standard test which is usually applied to processes in order to discover periodicities. As a matter of fact the standard test does not necessarily yield information about the frequencies or existence of periodicities.

The statistical reasoning underlying this test is described by the following argument. Assume that the data are samples of a random variable with variance  $\sigma^2$  whose sample functions are functions of time  $X(t)$ . We are considering that we might have obtained any one of an infinite number of possible sample functions and that the possible sample values  $X(n\Delta t)$ , denoted  $X_n$ , and  $X(n\Delta t + m\Delta t)$ , denoted  $X_{n+m}$ , have the joint probability density function

$$f(X_n, X_{n+m}) = \frac{1}{2\pi\sigma^2} \exp \left\{ - \left( \frac{X_n^2 - 2\rho X_n X_{n+m} + X_{n+m}^2}{2\sigma^2(1 - \rho^2)} \right) \right\}, \quad 6.1$$

where the correlation between  $X_n$  and  $X_{n+m}$  is  $\rho$ .

In this formulation it may be proved that the quantity,  $\rho$ , is an exponential function of the absolute value of the time difference,  $m\Delta t$ .<sup>(13)</sup> It is also possible to prove that the joint probability density of any  $k$  sample values is

multivariate normal.

In writing the density function as above we have implicitly assumed that the random process has zero expectation, a condition which can be approximated by subtracting the average value of the signal.

If the total length of the record is denoted by T and if  $\Delta t = T/N$  we may calculate the spectral density function of a given sample record as a function of radian frequency  $\omega_k$  by the formula

$$S_e(\omega_k) = \frac{2}{N\Delta t} \left| \sum_{n=1}^N X_n \exp \left\{ -j\omega_k n\Delta t \right\} \Delta t \right|^2. \quad 6.2$$

As may be shown this is equal to

$$S_e(\omega_k) = 4\Delta t \left[ \frac{R(0)}{2} + \sum_{m=1}^N \frac{N-m}{N} R(m) \cos(\omega_k m\Delta t) \right] \quad 6.3$$

which is related to the function computed on the digital computer.

We see that with different sample records we will obtain different functions  $S_e(\omega_k)$  so that for any particular value of radian frequency we can think of  $S_e$  as being a random variable with some probability distribution defined over the possible values of  $S_e$ . This random

variable is related to the set of random variables  $\{X_n\}$  where  $n$  ranges from 1 to  $N$  so that the probability distribution for  $S_e$  is related to the probability distribution for  $X_n$ . That is, in order to find the probability distribution for  $S_e$  we must know the probability distribution for  $X_n$ . This is the reason for assuming that the process  $X(t)$  is a Gaussian process.

As may be shown <sup>(14)</sup> the probability distribution for  $S_e$  is given by

$$f(S_e) = \frac{N}{2\sigma^2} \exp \left\{ -\frac{NS_e}{2\sigma^2} \right\}, \quad 6.4$$

where  $\sigma^2$  is the variance of the original process  $X(t)$ . With this probability distribution we may compute how likely any particular value of  $S_e$  is. In fact we may compute the probability that, for a particular value of radian frequency, say  $\omega_k$ ,  $S_e$  is less than some number  $C$ . This probability is

$$P\{S_e < C\} = \frac{N}{2\sigma^2} \int_0^C \exp \left\{ -\frac{NS_e}{2\sigma^2} \right\} dS_e = 1 - \exp \left( -\frac{NC}{2\sigma^2} \right). \quad 6.5$$

When analyzing the spectral estimates for a given record we are most interested in peak values of these estimates (i.e., the maximum value of the function  $S_e(\omega_k)$  over all values of  $\omega$ ). We would like to know what significance this peak has. In other words, we would like to calculate

a value C for which the following statement is true:

$$P \left\{ \max. \text{ over } \omega_k \text{ of } S_e(\omega_k) > C \right\} \leq 0.01 . \quad 6.6$$

This may be accomplished by computing the value of C for which

$$\int_{S_e(\omega_1) = 0}^{S_e(\omega_1) = C} \dots \int_{S_e(\omega_M) = 0}^{S_e(\omega_M) = C} f[S_e(\omega_1), \dots, S_e(\omega_M)]$$

$$dS_e(\omega_1) \dots dS_e(\omega_M) = 0.99 \quad 6.7$$

where  $f[S_e(\omega_1), \dots, S_e(\omega_M)]$  is the joint probability density function for the M values of  $S_e$  that have been estimated.

This joint probability density function is difficult to derive from the original probability density functions for  $X_n$  and  $X_{n+m}$  because of the fact that  $S_e(\omega_k)$  and  $S_e(\omega_l)$  are not necessarily independent random variables because the random variables  $X_n$  and  $X_{n+m}$  are not necessarily independent. However, for a set of carefully selected values of k it is theoretically possible to show that the random variables  $S_e(\omega_k)$  for k in this set are independent random variables. In that case the joint probability density function required in the integral above factors into the product of the separate probability density functions, and the integral factors

into the product of M identical integrals.

Finally the desired probability is

$$P \left\{ \max \text{ over } \omega_k \text{ of } S_e(\omega_k) > C \right\} = 1 - \left[ 1 - \exp \left( - \frac{NC}{2\sigma^2} \right) \right]^M \leq 0.01. \quad 6.8$$

This final relation may be solved for the desired value of C if the variance of the original process is known.

The test just described is a slight modification of the standard tests (see M. G. Kendall <sup>(14)</sup>) differing because there is no assumption made as to the independence of the original sample points. As indicated previously, if the sample points are widely spaced so that the sample points are statistically independent then we cannot estimate the spectral density function for frequencies sufficiently high as to be of great interest.

The test described above also differs from one described by Grenander and Rosenblatt <sup>(15)</sup> because the selected frequencies which may be used are different.

Finally the test described above has the drawbacks that the variance of the original process must be estimated (with unknown probability) and the expected value of the original process must be estimated (again with unknown probability) before the value of the confidence level may be computed.

On the credit side the test described above is independent of the correlation of the original sample points and hence, if the confidence level is exceeded we may infer that either the original process was not stationary and ergodic or that it was not Gaussian or both without having to include also the possibility that the original sample points were not independent.

#### 7. Statistical Properties of the Spectral Estimates

We need to investigate the statistical properties of the random variables  $S_e(\omega_k)$ . To do this we start by examining the properties of two functions

$$A(\omega_k) = \sqrt{\frac{2}{N\Delta t}} \sum_{n=1}^N X(n\Delta t) \cos(\omega_k n\Delta t) \Delta t \quad 7.1$$

and

$$B(\omega_k) = \sqrt{\frac{2}{N\Delta t}} \sum_{n=1}^N X(n\Delta t) \sin(\omega_k n\Delta t) \Delta t \quad 7.2$$

which are related to  $S_e(\omega_k)$  as below:

$$S_e(\omega_k) = A^2(\omega_k) + B^2(\omega_k). \quad 7.3$$

We should determine those values of  $\omega_k$  for which  $S_e(\omega_k)$  are a set of independent random variables.

We first note that  $A(\omega_k)$  and  $B(\omega_k)$  are composed of a linear combination of the random variables  $X_n$ . Since we have assumed that the random variables  $X_n$  are Gaussian we also have  $A(\omega_k)$  and  $B(\omega_k)$  as Gaussian random variables. Further, because they are Gaussian, we can establish the independence of  $A(\omega_k)$  and  $A(\omega_\ell)$  or  $B(\omega_n)$  simply by showing that the correlation between these random variables is zero. If the two random variables  $A(\omega_k)$  and  $B(\omega_k)$  are independent of the two random variables  $A(\omega_\ell)$  and  $B(\omega_\ell)$  then the random variables  $S_e(\omega_k)$  and  $S_e(\omega_\ell)$  must be independent.

An incidental result we should obtain in establishing the allowed values of  $\omega_k$  is an expression for the expectation of  $S_e(\omega_k)$  as a function of  $\omega$ . It is known that the expected value of the estimate approaches the true power spectral density as  $N$  approaches infinity. (16) However, the expected value for finite  $N$  would give us some idea of what variations we might expect in the spectral estimates over the entire set of frequencies.

We see that  $E[S_e(\omega_k)] = E[A^2(\omega_k)] + E[B^2(\omega_k)]$  and also we see that the correlation between  $A(\omega_k)$  and  $A(\omega_\ell)$  is given by

$$\rho_A = \frac{E[A(\omega_k) A(\omega_\ell)] - E[A(\omega_k)]E[A(\omega_\ell)]}{\sqrt{E[A^2(\omega_k)] E[A^2(\omega_\ell)]}}$$

so for both objectives we must compute the covariance,  $\sigma_{k\ell}$ , of the random variables  $A(\omega_k)$ ,  $A(\omega_\ell)$ ,  $B(\omega_k)$  and  $B(\omega_\ell)$ .

The expectation of the product of  $A(\omega_k)$  and  $A(\omega_\ell)$  is

$$\begin{aligned} E[A(\omega_k) A(\omega_\ell)] &= E \left\{ \frac{2}{N\Delta t} \left[ \sum_{n=1}^N X(n\Delta t) \cos(\omega_k n\Delta t) \right] \right. \\ &\quad \left. \left[ \sum_{j=1}^N X(j\Delta t) \cos(\omega_\ell j\Delta t) \right] \right\} \\ &= \frac{2}{N\Delta t} \sum_{n,j=1}^N E[X(n\Delta t) X(j\Delta t)] \cos(\omega_k n\Delta t) \cos(\omega_\ell j\Delta t). \end{aligned} \quad 7.5$$

If the process is ergodic and if  $E[X(n\Delta t)]$  is zero we have  $E[X(n\Delta t) X(j\Delta t)]$  as the covariance,  $\sigma_{k\ell}$ , and also the equality

$$\begin{aligned} \sigma_{k\ell} &= E[A(\omega_k) A(\omega_\ell)] \\ &= \frac{2\sigma^2}{N\Delta t} \sum_{n,j=1}^N \rho(|n-j|\Delta t) \cos(\omega_k n\Delta t) \cos(\omega_\ell j\Delta t) \end{aligned} \quad 7.6$$

where  $\sigma^2$  is the variance of the  $X(t)$  process and  $\rho$  is the correlation between  $X(n\Delta t)$  and  $X(j\Delta t)$ . As stated before, if the process is a Markov Gaussian process it

can be proved that  $\rho$  has the form

$$\rho = \exp \left\{ - \frac{|n-j|\Delta t}{\tau} \right\} \quad 7.7$$

where  $\tau$  is a constant dictated by how wide a frequency band the original process occupies.

By rearranging the order of summation we can obtain

$$\sigma_{k\ell} = \frac{4\sigma^2}{N\Delta t} \sum_{u=1}^{N-1} \sum_{X=u+1}^N \rho(u\Delta t) \cos(\omega_k X\Delta t) \cos[\omega_\ell(X-u)\Delta t] \quad 7.8$$

and then by the use of trigonometric identities we have

$$\sigma_{k\ell} = \frac{2\sigma^2}{N\Delta t} \sum_{u=1}^{N-1} \sum_{X=u+1}^N \rho(u\Delta t) \left\{ \cos[X(\omega_k + \omega_\ell)\Delta t - \omega_\ell u\Delta t] + \cos[(\omega_k - \omega_\ell)X\Delta t + \omega_\ell u\Delta t] \right\} \quad 7.9$$

which may be evaluated to give

$$\sigma_{k\ell} = \frac{2\sigma^2}{N\Delta t} \sum_{u=1}^{N-1} \rho(u\Delta t) \left\{ \frac{\cos[(N+1)\alpha + u\beta] \sin[(N-u)\alpha]}{\sin \alpha} + \frac{\cos[(N+1)\beta + u\alpha] \sin[(N-u)\beta]}{\sin \beta} \right\} \quad 7.10$$

where

$$\alpha = \frac{(\omega_k + \omega_\ell)}{2} \Delta t, \quad \beta = \frac{(\omega_k - \omega_\ell)}{2} \Delta t. \quad 7.11$$

If  $\rho(t)$  is known then the last sum can be evaluated

but it is advantageous to examine the terms as they stand. Upon examination of the auto-correlation estimates, Figures 3 and 4, it appears probable that the true correlation drops to zero in a time less than one second; hence,  $\tau$  is less than one. This means approximately the first five terms in the sum are the significant terms.

We cannot expect to estimate the spectrum for frequencies higher than the frequency for which we have two sample points per cycle. This means that the maximum value of  $\alpha$  was chosen to be

$$\text{Max. } (\omega_k \Delta t) = \frac{2\pi \Delta t}{T_k} \leq \frac{2\pi \Delta t}{2\Delta t} = \pi \quad 7.12$$

so that  $\alpha$  lies between  $\pi$  and zero. In fact we have chosen our sampling time so that  $\alpha$  lies between  $\pi/2$  and zero.

As  $\alpha$  approaches zero we see that the sum approaches

$$\sum_{u=1}^{\text{small } u} \rho(u\Delta t) \left\{ \frac{\cos(N\alpha)\sin(N\alpha)}{\sin \alpha} + \frac{\cos(N\beta)\sin(N\beta)}{\sin \beta} \right\} \quad 7.13$$

or

$$\sum_{u=1}^{\text{small } u} \rho(u\Delta t) \frac{1}{2} \left\{ \frac{\sin(2N\alpha)}{\sin \alpha} + \frac{\sin(2N\beta)}{\sin \beta} \right\}. \quad 7.14$$

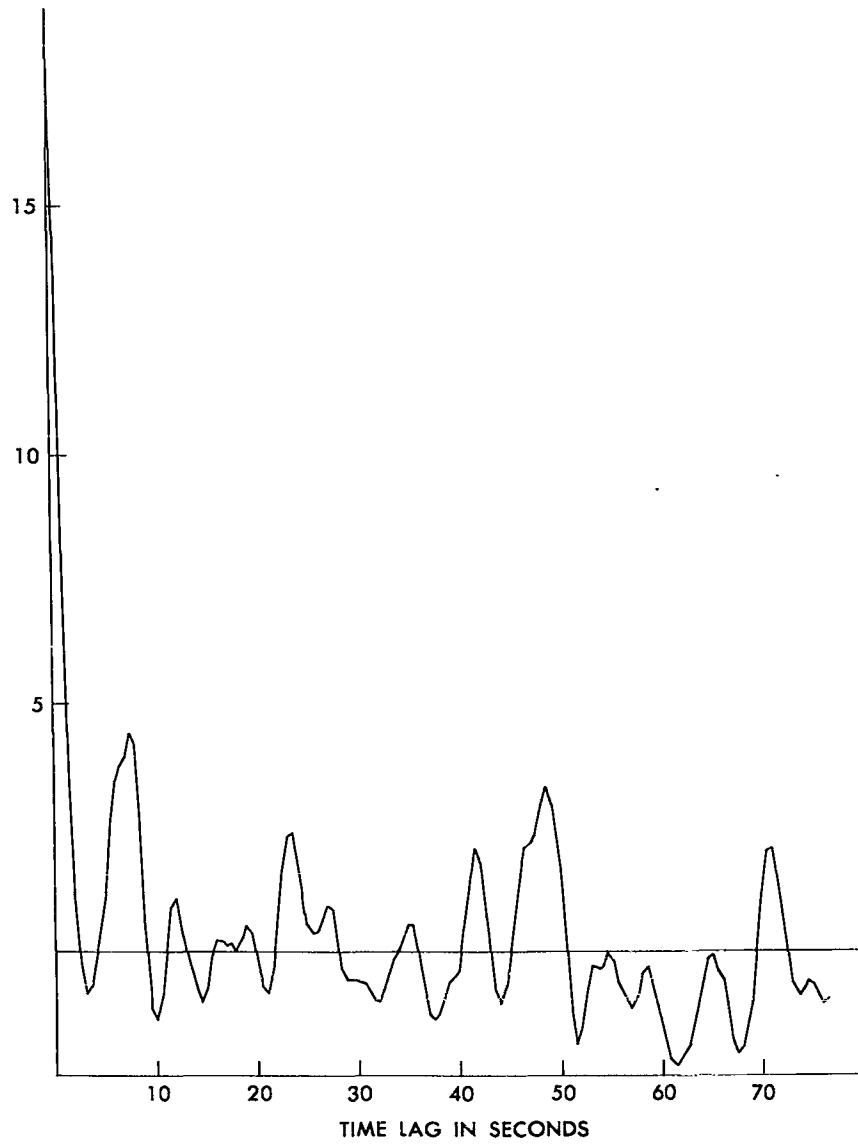


Fig. 3. Auto-correlation function of the detected 17.9 mc signal from 1431:18 to 1436:20 PST, August 4, 1960.

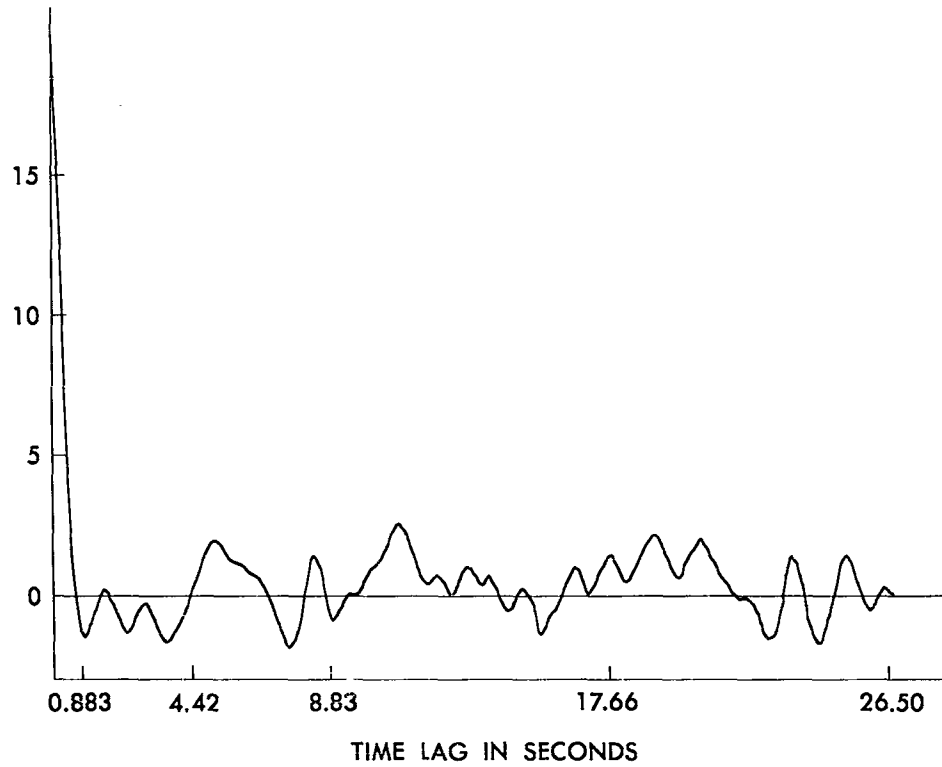


Fig. 4. Auto-correlation function of the detected 11.9 mc signal from 1616:09 to 1618 PST, June 15, 1960.

Consequently we would expect the cross correlation to fluctuate as a function of  $\alpha$  and  $\beta$  between zero and some large number whose magnitude is less than

$$\frac{2\sigma^2}{\Delta t} \sum_{u=1}^{\text{small } u} \rho(u\Delta t) \text{ and whose magnitude varies as}$$

$\left\{ \frac{1}{\sin(\alpha)} \right\} + \left\{ \frac{1}{\sin(\beta)} \right\}$  as  $N\alpha$  and  $N\beta$  pass through the points  $M\pi$  and  $(2M+1)\pi/2$  ( $\sin N\alpha = 0$  and  $\sin N\alpha = 1$ ).

The expected value of  $S_e(\omega_k)$  depends upon  $\sigma_{kk}$  and we see that  $\sigma_{kk}$  is given by the Eq. 7.10 where  $\beta$  is zero and  $\alpha$  is  $\omega_k \Delta t$ . In that case we have

$$\sigma_{kk} = \frac{2\sigma^2}{N\Delta t} \sum_{u=1}^{\text{small } u} \rho(u\Delta t) \left\{ \frac{\cos[(N+1)\alpha] \sin[(N-u)\alpha]}{\sin \alpha} + \cos(u\alpha) \right\} \quad 7.15$$

and it is apparent that this fluctuates wildly as a function of  $\alpha = \omega_k \Delta t$  for small  $\alpha$ .

To find the allowed values of  $\omega_k$  the summation should be performed and the resulting transcendental expression should be set to zero. Then the resulting equation should be solved for the allowed values,  $\{\omega_k\}$ .

One of the conclusions to be drawn from this analysis is that the value of the minimum frequency at which the spectral density is estimated should be greater than the

frequency for which  $\omega_k \Delta t$  is about five or ten degrees.

If the process contains periodicities (as might be the case when two modes of propagation exist simultaneously) we would expect peaks occurring in the spectral estimates at the frequencies of the periodicities. The width of these peaks would be related to the duration of the periodic component or to the duration of the record, whichever was shorter. The purpose behind not smoothing the spectral estimates by the use of a weighting function in the data was to produce the narrowest possible peaks from these periodicities.

Suppose that the record lasted for T seconds and that it contained a sinusoidal component that lasted for L seconds where T is the order of five or ten times L and where there are not less than about five cycles of sinusoidal fade in evidence. We then can characterize the received signal amplitude as being the sum of a sinusoidal function and a random function, X(t), as follows:

$$f(t) = A \sin(at) U(t) U(L - t) + X(t) \quad 7.16$$

where U(t) is a unit step function. In that case it can be shown that the expected value of the spectral

estimate is approximately

$$E[S(k\Delta g)] \approx \frac{A^2 L^2}{8T} \left\{ \left[ \frac{\sin\left(\frac{n\omega_0 + a}{2} L\right)}{\frac{n\omega_0 + a}{2} L} \right]^2 + \left[ \frac{\sin\left(\frac{n\omega_0 - a}{2} L\right)}{\frac{n\omega_0 - a}{2} L} \right]^2 \right\} + \int_0^{T/4} \rho(\tau) \cos(n\omega_0 \tau) d\tau \quad 7.17$$

where the first term is due to the sinusoid. This expression displays the peaks mentioned above.

The identification of these peaks remains a problem whose solution depends upon a more complete knowledge of the possible variations of the spectral estimates. Knowledge of the values of  $\omega$  at which the cross-correlation between spectral estimates is zero would help considerably; however, the worth of pursuing this line of work is questionable.

The digital computations are more accurate than the analog computations, but this appears to be the only advantage the digital computer program has over the analog computer program. Unfortunately the length of time required to compute spectral density estimates with the digital computer increases approximately with the square of the number of data points. The five minute sample of data used for the estimate shown in Figure 8 (page 47)

contained 600 points and required 4.6 minutes of computer time. The full 22 minutes of data in this particular sample would require about an hour and a half of computer time. At this rate the IBM 704 computer would require about 9.3 hours to analyze a 55 minute sample such as has been analyzed with the analog computer in about one hour.

Because the analog computer can handle longer samples of data the power spectral density estimates are considerable more stable; that is, they don't fluctuate as Eq. (7.15) predicts that the digital computer estimates will fluctuate. This fluctuation is shown in Figure 8 where the digital computer estimate of the power spectral density for data in the time interval of 1431:18 to 1436:20 PST on August 4, 1960 is graphed along with the analog computer estimate of the power spectral density for the data in the time period from 1421 to 1443 PST on August 4, 1960.

The relative calibration between the amplitudes of the two estimates is unknown so only the general shape of the curves can be compared. When comparing the two curves one must keep in mind that the digital computer estimate is for five minutes of the data whereas the analog computer estimate is for the whole 22 minutes.

8. Analog Computer Program

The purpose of the analog computer program is to obtain spectral estimates from the sample functions and to identify periodic fades and to obtain the following information concerning these periodic fades: (1) the duration time, (2) the starting and ending time, (3) their variation in 'frequency' and (4) their amplitude.

To obtain this information from a known sample function,  $e_s(t)$ , the analog computer is programmed to solve the second-order equation

$$e_o'' + 2\sigma e_o' + (\omega^2 + \sigma^2) e_o = \omega^2 e_s \quad 8.1$$

where  $\omega$  and  $\sigma$  are constants that are adjusted by changing a dc voltage in the computer. The voltage,  $e_o(t)$ , is then similar to the output of a tuned circuit that has been excited by the voltage  $e_s(t)$ . The average of the square of the voltage,  $e_o(t)$ , is computed as a measure of the power density in  $e_s(t)$  at the frequency  $\omega$ . A diagram of the computer circuit is shown in Figure 5.

The data are treated in the following way. The signal is recorded on magnetic tape at 0.075 inches per second and then played back at 7.5 inches per second



and re-recorded on a 25 foot loop of magnetic tape. Thus, the time scale is compressed by a factor of 100. Along with the data a synchronizing signal which occurs at the same time as the start of the data is recorded on an adjacent channel of the magnetic tape. This tape is then reproduced with a loop-tape magazine so that the data are reproduced over and over again in a repetitive fashion.

On the first reproduction of the data the voltage out of the magnetic tape recorder is squared in the analog computer and is put into the simulated resonant circuit of the computer. The simulated resonant circuit is tuned to a low frequency of, say, one cps. The synchronizing signal starts a pre-set timing circuit in the computer. Samples of the computer outputs are shown in Figure 6.

At the end of the first reproduction of the data the computer de-energizes its circuits, reads out the average of the square of the response of the simulated tuned circuit and resets the tuning of the tuned circuit to a higher frequency, say, 1.08 cps. At the start of the second reproduction of the data the synchronizing signal re-activates the computer circuits and the cycle is repeated. In this fashion a measure of the power density is obtained for frequencies spaced throughout the range from 0.01 cps to 1 cps (as reckoned on the time scale of the original data).

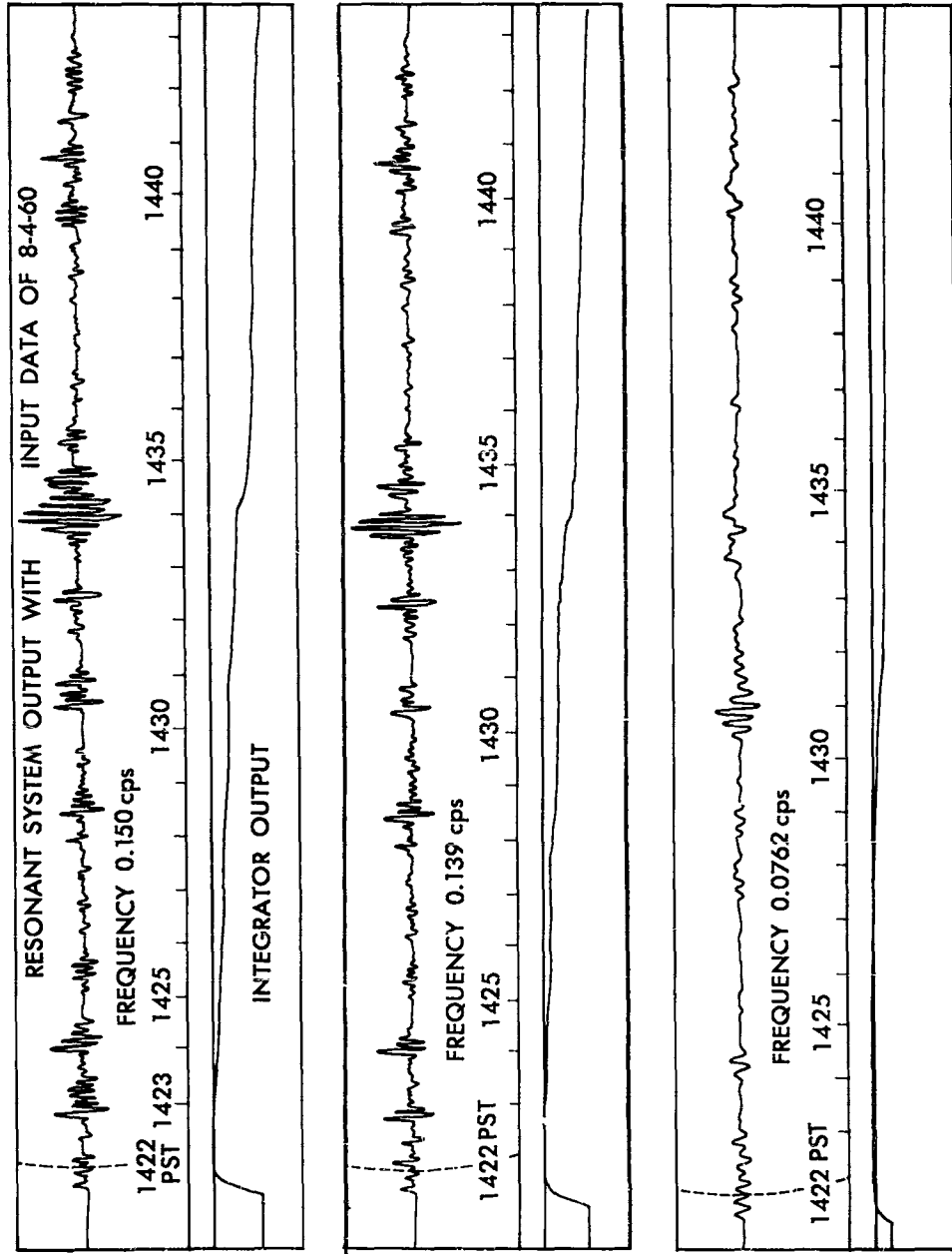


Fig. 6. Analog computer output voltages.

In order to briefly outline the properties of the spectral estimates obtained from the analog computer we may analyze the differential equation which the computer solves. This equation is

$$e_o'' + 2\sigma e_o' + (\omega_o^2 + \sigma^2) e_o = \omega_o^2 e_s \quad 8.2$$

where  $e_s$  is the square of the data waveform and  $e_o$  is a voltage yielding a measure of the power density. If  $e_s$  were a sinusoid of frequency  $\omega_1$  the voltage  $e_o$  would approach a sinusoid. We may find this sinusoid by finding the steady state solution of the differential equation by solving the equation

$$-\omega_1^2 \dot{E}_o + 2j\omega_1\sigma \dot{E}_o + (\omega_o^2 + \sigma^2) \dot{E}_o = \omega_o^2 \dot{E}_s \quad 8.3$$

Solution of this equation gives us

$$E_o = \frac{\omega_o^2 E_s}{\sqrt{(\omega_o^2 + \sigma^2 - \omega_1^2)^2 + (2\omega_1\sigma)^2}} \quad 8.4$$

where  $E_o$  is the magnitude of the sinusoidal voltage  $e_o$ . We may find the peak value of the response when the frequency is varied by taking the derivative of this expression with respect to  $\omega_1$  and then by setting this derivative equal to zero. The result of this is that the response  $E_o$  is maximum at  $\omega_1 = \sqrt{\omega_o^2 - \sigma^2}$ . When this condition is met the formula for  $E_o$  may be rewritten as

$$E_o = \sqrt{2} \frac{QE_s}{\sqrt{1 + \frac{1}{2Q^2}}} \approx \sqrt{2} QE_s, \quad 8.5$$

where  $Q = \frac{\omega_o}{2\sigma}$  and we see that we can change the tuning of the resonant system without changing the ratio of  $E_o/E_s^2$  if the  $Q$  is kept constant. The analog computer was set so that  $Q = 2\pi$  for the present data. With this or higher values of  $Q$  we have the resonant frequency of the system  $\sqrt{\omega_o^2 - \sigma^2}$  equal to  $\omega_o$  within 1.5%. The change in tuning of the resonant system which is made between runs of the data is made as a percentage of the previous resonant frequency. The frequency increment added to the resonant frequency is equal to one half of the bandwidth of the tuned system. Because of this way of changing frequency the resultant plots of power density versus frequency are made on logarithmic graph paper.

If  $e_s$  is some function other than a periodic function we may find an integral solution of the differential equation by the use of the Laplace transform. Solving by the use of the Laplace transform and using the information that  $e_o(0)$  and  $e_o'(0)$  are both equal to zero, we find that

$$E_o(s) = \frac{\omega_o^2 E_s(s)}{s^2 + 2\sigma s + (\omega_o^2 + \sigma^2)}. \quad 8.6$$

Inverting this expression with the use of the convolution integral, we obtain an integral form of the solution

$$e_o = \omega_o^2 \int_0^t e_s(\lambda) \exp[-\sigma(t-\lambda)] \sin[\omega_o(t-\lambda)] d\lambda . \quad 8.7$$

This is an exact expression for the computed voltage during the time the computer is 'tuned' to the frequency  $\omega_o$ .

#### 9. Expected Value of the Spectral Estimates

The measure of power density contained in a given record at a frequency  $\omega$  is computed in the computer by the following formula

$$S_e = \left(\frac{1}{\omega T}\right) \int_0^T e_o^2(t) dt. \quad 9.1$$

We use this number as an estimate of the power density of the true power spectrum of the random process which produced the data record. In order to decide whether this is a good estimate of the value of the true power spectrum we may compute the expected value of  $S_e$  and discover how the power density of any given record is related to the true power spectrum.

In finding the expectation of  $S_e$  we regard the input signal  $e_s(t)$  as a random variable so that we are

averaging over all inputs that we might possibly get from the random process with the spectral density  $F(\omega)$ . The desired expected value is obtained from the calculation

$$E [S_e] = \frac{1}{\omega T} \int_0^T E [e_o^2(t)] dt. \quad 9.2$$

Hence, we must compute

$$E [e_o^2(T)] = E \left\{ \left[ \omega^2 \int_0^t e_s(\lambda) \exp [-\sigma(t-\lambda)] \sin [\omega(t-\lambda)] d\lambda \right] \cdot \left[ \omega^2 \int_0^t e_s(\tau) \exp [-\sigma(t-\tau)] \sin [\omega(t-\tau)] d\tau \right] \right\}. \quad 9.3$$

Combining this into a double integral and then using trigonometric identities and the following definition of the correlation function

$$\rho(\lambda-\tau) = \frac{E [e_s(\lambda) e_s(\tau)] - E^2 [e_s(t)]}{\sigma_x^2} \quad 9.4$$

where  $\sigma_x^2$  is equal to  $E [e_s^2(t)] - E^2 [e_s(t)]$  and where  $E^2 [e_s(t)]$  is assumed to be zero, we can rewrite the expected value as

$$E [e_o^2(t)] = \frac{\omega^2 \sigma_x^2}{2} \int_0^t \int_0^t \rho(\lambda-\tau) \exp [\sigma(\lambda+\tau-2t)] \cdot [\cos \omega(\lambda-\tau) - \cos \omega(\lambda+\tau-2t)] d\tau d\lambda. \quad 9.5$$

The variables of integration in the above double

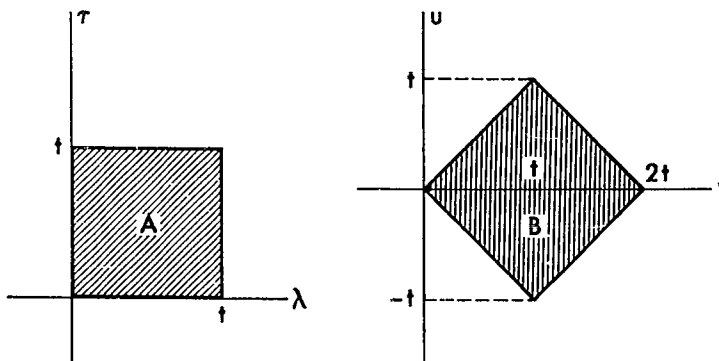
integral may be transformed with the following transformation and its inverse

$$\begin{aligned} u &= \lambda - \tau & \tau &= 1/2(v+u) \\ v &= \lambda + \tau & \lambda &= 1/2(v-u) \end{aligned} \quad 9.6$$

which has the Jacobian

$$\left| \frac{\delta(\tau, \lambda)}{\delta(u, v)} \right| = 1/2 . \quad 9.7$$

This transformation maps the shaded area A in the first diagram into the shaded area B in the following right-hand diagram.



Under this transformation the integral becomes

$$\begin{aligned} E \left[ e_o^2(t) \right] &= \frac{\omega^2 \sigma^2}{4} \exp(-2\sigma t) \int_0^t \exp(\sigma v) \int_{-v}^v \rho(u) \cos(\omega u) \, du \, dv \\ &- \frac{\omega^2 \sigma^2}{4} \exp(-2\sigma t) \int_0^t \exp(\sigma v) \cos[\omega(v-2t)] \int_{-v}^v \rho(u) \, du \, dv \\ &+ \frac{\omega^2 \sigma^2}{4} \exp(-2\sigma t) \int_t^{2t} \exp(\sigma v) \int_{-2t+v}^{2t-v} \rho(u) \cos(\omega u) \, du \, dv \\ &- \frac{\omega^2 \sigma^2}{4} \exp(-2\sigma t) \int_t^{2t} \exp(\sigma v) \cos[\omega(v-2t)] \int_{-2t+v}^{2t-v} \rho(u) \, du \, dv \quad 9.8 \end{aligned}$$

So that we may relate this expression to the power spectrum of the random process we substitute for the correlation function the following relation

$$\rho(u) = 2 \int_0^{\infty} F(\omega_1) \cos(\omega_1 u) d\omega_1$$

We can then invert the order of integration and evaluate the resulting integrals to obtain

$$\begin{aligned} E[e_o^2(t)] &= \frac{\omega^2 \sigma_x^2}{2} \exp(-2\sigma t) \left\{ \int_0^{\infty} F(\omega_1) \left( \frac{1}{\sigma^2 + (\omega_1 + \omega)^2} \right. \right. \\ &+ \left. \frac{1}{\sigma^2 + (\omega_1 - \omega)^2} \right) d\omega_1 - \int_0^{\infty} \frac{F(\omega_1)}{\omega_1} \frac{\sigma \sin(2\omega t) + (\omega_1 + \omega) \cos(2\omega t)}{\sigma^2 + (\omega_1 + \omega)^2} d\omega_1 \\ &+ \left. \int_0^{\infty} \frac{F(\omega_1)}{\omega_1} \frac{\sigma \sin(2\omega t) - (\omega_1 - \omega) \cos(2\omega t)}{\sigma^2 + (\omega_1 - \omega)^2} d\omega_1 \right\} \\ &+ \frac{\omega^2 \sigma_x^2}{2} \exp(-\sigma t) \left\{ \int_0^{\infty} F(\omega_1) \frac{\sigma \sin[(\omega_1 + \omega)t] - (\omega_1 + \omega) \cos[(\omega_1 + \omega)t]}{(\omega_1 + \omega) [\sigma^2 + (\omega_1 + \omega)^2]} d\omega_1 \right. \\ &+ \int_0^{\infty} \frac{F(\omega_1)}{\omega_1} \frac{\sigma \sin[(\omega_1 - \omega)t] - (\omega_1 - \omega) \cos[(\omega_1 - \omega)t]}{(\omega_1 - \omega) [\sigma^2 + (\omega_1 - \omega)^2]} d\omega_1 \\ &- \int_0^{\infty} \frac{F(\omega_1)}{\omega_1} \frac{\sigma \sin[(\omega_1 - \omega)t] - (\omega_1 + \omega) \cos[(\omega_1 - \omega)t]}{\sigma^2 + (\omega_1 + \omega)^2} d\omega_1 \\ &- \int_0^{\infty} \frac{F(\omega_1)}{\omega_1} \frac{\sigma \sin[(\omega_1 + \omega)t] - (\omega_1 - \omega) \cos[(\omega_1 + \omega)t]}{\sigma^2 + (\omega_1 - \omega)^2} d\omega_1 \\ &- \left. \int_0^{\infty} \frac{F(\omega_1)}{\omega_1} \frac{\sigma \sin[(\omega_1 + \omega)t] + (\omega_1 + \omega) \cos[(\omega_1 + \omega)t]}{(\omega_1 + \omega) [\sigma^2 + (\omega_1 + \omega)^2]} d\omega_1 \right\} \end{aligned}$$

$$\begin{aligned}
& - \int_0^{\infty} F(\omega_1) \frac{\sigma \sin [(\omega_1 - \omega)t] + (\omega_1 - \omega) \cos [(\omega_1 - \omega)t]}{[\omega_1 - \omega)(\sigma^2 + (\omega_1 - \omega)^2]} d\omega_1 \\
& + \int_0^{\infty} \frac{F(\omega_1)}{\omega_1} \frac{\sigma \sin [(\omega_1 + \omega)t] + (\omega_1 + \omega) \cos [(\omega_1 + \omega)t]}{\sigma^2 + (\omega_1 + \omega)^2} d\omega_1 \\
& + \int_0^{\infty} \frac{F(\omega_1)}{\omega_1} \frac{\sigma \sin [(\omega_1 - \omega)t] + (\omega_1 - \omega) \cos [(\omega_1 - \omega)t]}{\sigma^2 + (\omega_1 - \omega)^2} d\omega_1 \Bigg\} \\
& + \frac{\omega^2 \sigma^2}{2} \int_0^{\infty} F(\omega_1) \left[ \frac{\omega/\omega_1}{\sigma^2 + (\omega_1 - \omega)^2} - \frac{\omega/\omega_1}{\sigma^2 + (\omega_1 + \omega)^2} \right] d\omega_1 . \tag{9.10}
\end{aligned}$$

In this expression the first three terms have the factor  $\exp(-2\sigma t)$ , the next eight terms have the factor  $\exp(-\sigma t)$  but the last term contains no such factor. The significance of this fact is that after ten cycles of the desired frequency each of the first eleven terms is multiplied by a factor that is less than 0.01. When the records are about twenty cycles or more of the desired frequency in length we may approximate the expression for the expected value with just the last term of the foregoing equation. Then the expected value of the spectral estimate is

$$\begin{aligned}
E [S_e(\omega)] & \approx \frac{\sigma^2}{2\omega} \int_0^{\infty} F(\omega_1) \frac{\omega}{\omega_1} \left[ \frac{1}{\frac{1}{4Q^2} + \left(\frac{\omega_1}{\omega} - 1\right)^2} \right. \\
& \left. - \frac{1}{\frac{1}{4Q^2} + \left(\frac{\omega_1}{\omega} + 1\right)^2} \right] d\omega_1 . \tag{9.11}
\end{aligned}$$

The integrand in this expression is a product of the function describing the power spectrum,  $F(\omega_1)$ , and a weighting function. A plot of the weighting function is shown in Figure 7. The weighting function has a peak at the frequency at which the spectrum is being estimated and drops rapidly to zero on either side of this peak. If we define the side frequencies as those frequencies at which this plot is down by 1/2, we see that we have a 'bandwidth' of roughly  $1/Q$  where  $Q$  is the figure of merit of the simulated tuned circuit.

This form of weighting function assures that the greatest contribution to the expected value of the estimate comes from  $F(\omega_1)$  in the neighborhood of the frequency of the estimate.

As a check on the work we may compute the form of the estimate for special types of  $F(\omega_1)$ . If the true power spectral density function is a constant,  $A$ , over the whole spectrum then the expected value of the estimate is

$$E [S_e(\omega)] = (\sigma_x^2/2\omega) \int_0^\infty A (\omega/\omega_1) \left[ \frac{1}{\frac{1}{4Q^2} + \left(\frac{\omega_1}{\omega} - 1\right)^2} - \frac{1}{\frac{1}{4Q^2} + \left(\frac{\omega_1}{\omega} + 1\right)^2} \right] d\omega_1 .$$

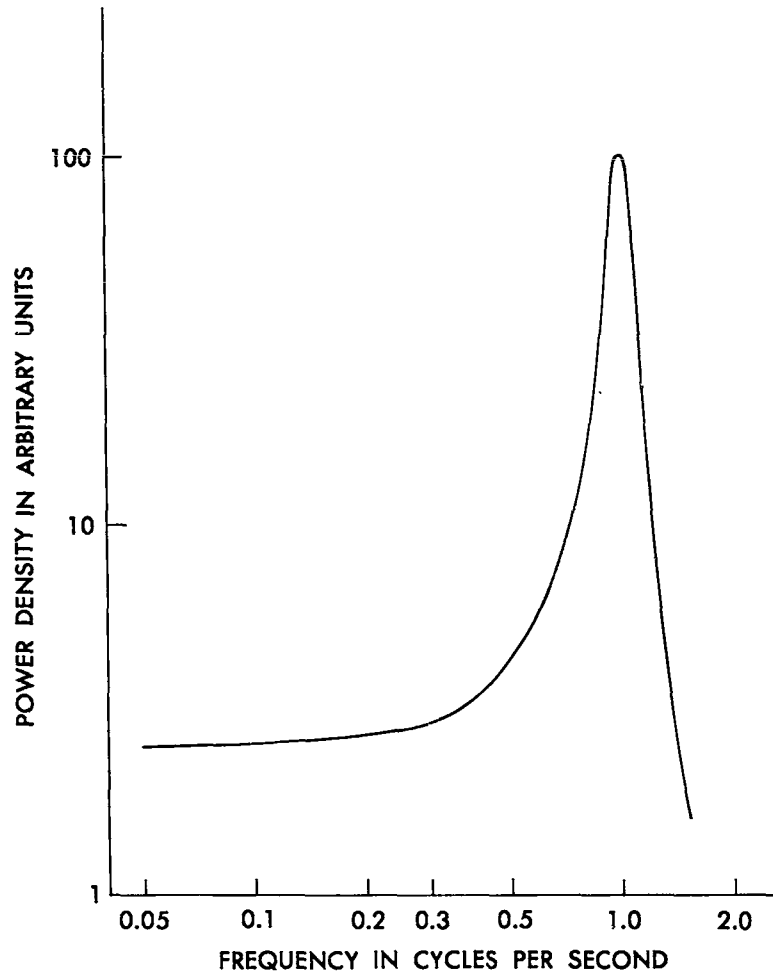


Fig. 7. Weighting function in  $E [S_e(\omega)]$ .

Then we may change variables as per the relations

$$\omega_1/\omega = u, \quad d\omega_1 = \omega du \quad 9.13$$

and the expected value of the estimate becomes

$$E(S_e) = - (A\sigma_x^2/2) \int_0^\infty (1/u) \left[ \frac{1}{(u-1)^2 + \frac{1}{4Q^2}} - \frac{1}{(u+1)^2 + \frac{1}{4Q^2}} \right] du. \quad 9.14$$

Since  $\omega$  does not appear in the integral the estimate is a constant proportional to the true value of the spectrum.

## 10. Results

Two samples of the data for which spectral estimates have been made are shown in Figures 1 and 2. The first sample in Figure 1 is a recording of the detected voltage from a Collins 51J4 receiver lasting for 22 minutes obtained on August 4, 1960. The receiver was adjusted so that the detected voltage was directly proportional to the r.f. signal voltage. The signal was received at 17.9 mc over a 6000 km path arriving at approximately 13 degrees south of east. The second sample in Figure 2 is a recording of the detected voltage from the IF of a Collins 75S1 receiver lasting for 56 minutes obtained on May 9, 1962. Again the detected voltage is proportional to the input signal. The signal (WWV) was received at 20 mc over a 3710 km path arriving at an angle of about 2 degrees north

of east. The direction of increasing signal strength in Figure 1 is downward whereas it is upward in Figure 2.

In both samples there is considerable variation in the amplitude of the received signal. The signal actually fell below the noise level of the receiver on occasion. However, the rate of variation is not excessive. The fades do not exceed one cycle per second in either sample. In a few cases (not analyzed) fades of one to two cycles per second have been observed.

The first data sample appears to contain no fades which could be described as being caused by a beat between signals arriving via two modes of propagation. The second sample has such fades, one occurring between 0030 and 0035 GMT. There appears to be a definite beat of 0.3 cycles per second lasting for tens of cycles. Another appears between 0039 and 0041 GMT with a frequency of 0.15 cps. Both of these beats appear to be superimposed onto a slower type of fade which has larger peak values.

The data in Figure 2 contain many peaks of signal lasting 20 and 30 seconds. Between 2355 and 2358 GMT there appears to be a periodic increase of signal with a frequency of approximately 0.025 cps. On the other hand, this type of fade is lacking in the data shown in Figure 1.

Wild and Roberts<sup>(3)</sup> observed that some of their scintillation data appeared to be caused by a single lens-like irregularity in ionization which caused a single large increase in the signal received. It is possible that a similar situation accounts for the longer lasting peaks of signal strength in the present data.

The spectral density estimates computed with the IBM 704 digital computer are shown in Figures 8 and 9. The estimate shown in Figure 8 is for a five minute section of the data shown in Figure 1. The time interval of the section analyzed lies between 1431:18 and 1436:20 PST. The estimate of the spectral density function is the solid-line curve. The estimate shown in Figure 9 is for data taken on June 15, 1960, from 1616:09 to 1618 PST. These data are a recording of the signal voltage out of the detector of a R390A/URR receiver mentioned in the equipment appendix. The signal was transmitted over a 6000 km path at 11.9 mc.

Both of these estimates exhibit the large fluctuation at low frequencies which tends to drop off at higher frequencies, say 0.2 cps. If these fluctuations are caused solely by the rectangular truncation of the data they should have a period of 0.0131 cps for the estimate in Figure 8 and a period of 0.038 cps for the estimate in Figure 9. This period is directly related to the time

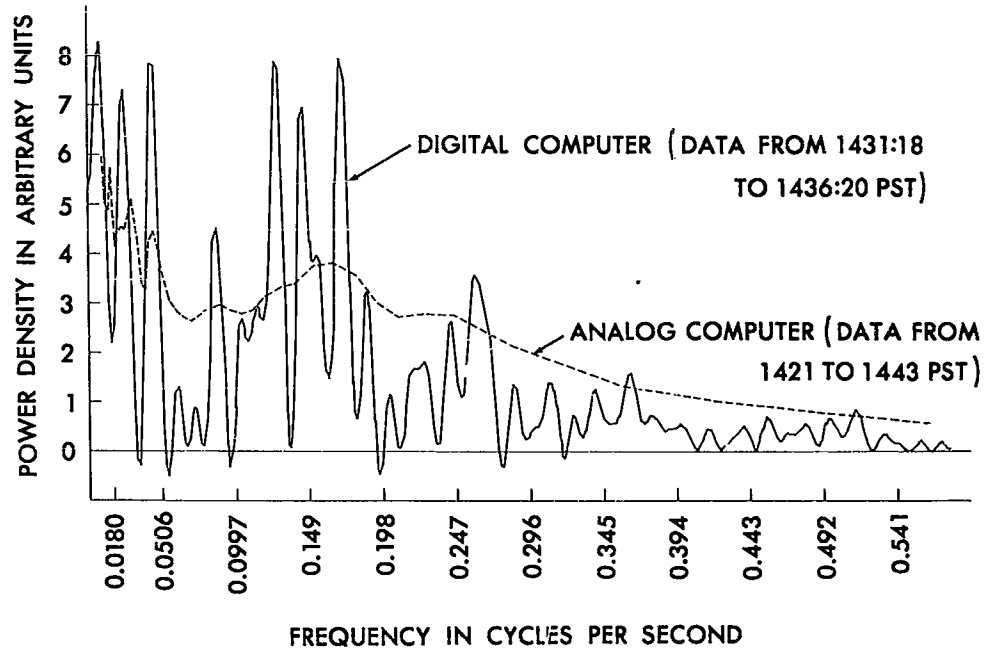


Fig. 8. Power spectral density estimate of the fading power in the detected 17.9 mc signal, August 4, 1960, as computed by digital and analog methods.

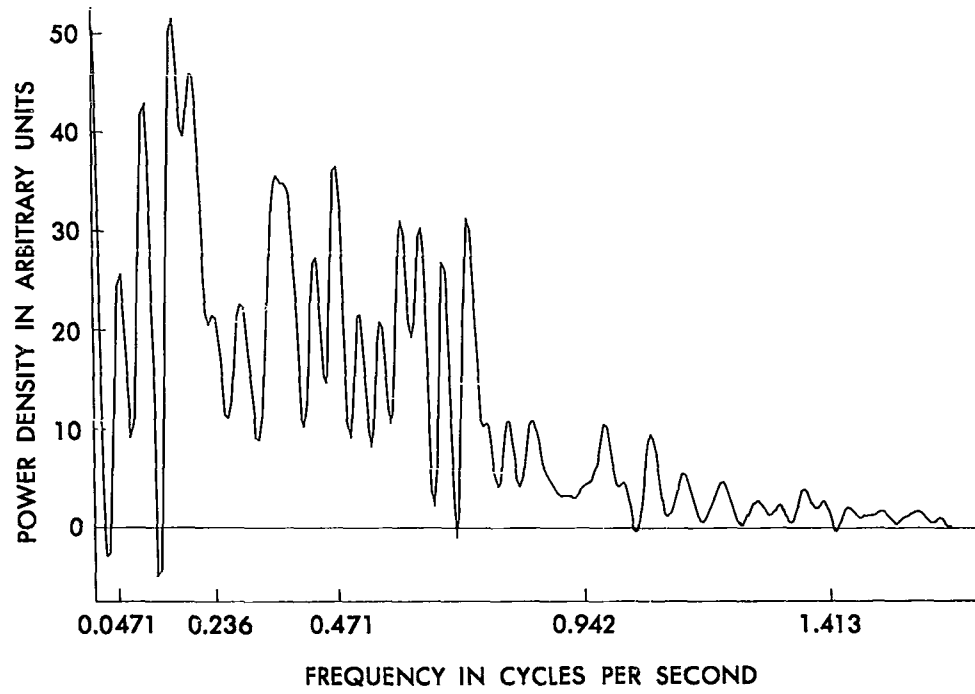


Fig. 9. Power spectral density estimate of the fading power in the detected 11.9 mc signal from 1616:09 to 1618 PST, June 15, 1960.

length of the auto-correlation function computed for the records. Since this is computed for a time period of one-fourth of the length of the record (see equation (5.1)) we can compute the period of the oscillations.

There are two peaks in the estimate of Figure 8 which appear to be wider than the remaining peaks, one at about 0.115 cps and one at about 0.26 cps. These peaks have a width at their bases of approximately 0.04 cps and 0.035 cps respectively. If these peaks were caused by sinusoids (or quasi-sinusoids) we may measure their effective width and compute a value for the quantity  $L$  in equation (7.17) where  $L$  is the duration time of the sinusoid. On this basis the sinusoids must have lasted about 25 seconds and 30 seconds respectively. That would correspond to 3 cycles and 8 cycles of the respective frequencies. This interpretation of these peaks is not satisfactory as one can see when inspecting the raw data (Figure 1). The analog computer estimates are considerable more useful since they do not fluctuate as wildly.

The spectral estimate shown in Figure 9 shows power density at considerably higher frequencies than that of Figure 8. Unfortunately the data for this sample exist only in the form of punched cards (not on magnetic tape) and hence, cannot be readily analyzed on the analog computer.

When computing the spectral density estimates with the digital computer the auto-correlation function is also computed. The auto-correlation functions for the data of August 4, 1960, from 1431:18 to 1436:20 PST and of June 15, 1960, from 1616:09 to 1618 PST are shown in Figures 3 and 4. These plots both start out at a value equal to the mean-square value of the data (zero time lag). The curves then drop rapidly to zero and thereafter oscillate randomly about zero. Data points separated in time by a period greater than the time required for the auto-correlation curve to drop to zero are more likely to be statistically independent. The sustained oscillations are apparently indicative of a periodic process.

The most informative and useful graphs are the power spectral density estimates computed with the analog computer. These are shown in Figures 10 through 15. All except one of these estimates start dropping off to zero in the neighborhood of 0.2 cps and increase or stay constant below this frequency, showing that the power density of the fades lies below 0.2 cps. Actually there is power density at much lower frequencies, say one to three orders of magnitude below 0.02 cps since the signal fades in and out over hour periods and since the signal has a strong periodic component with a period

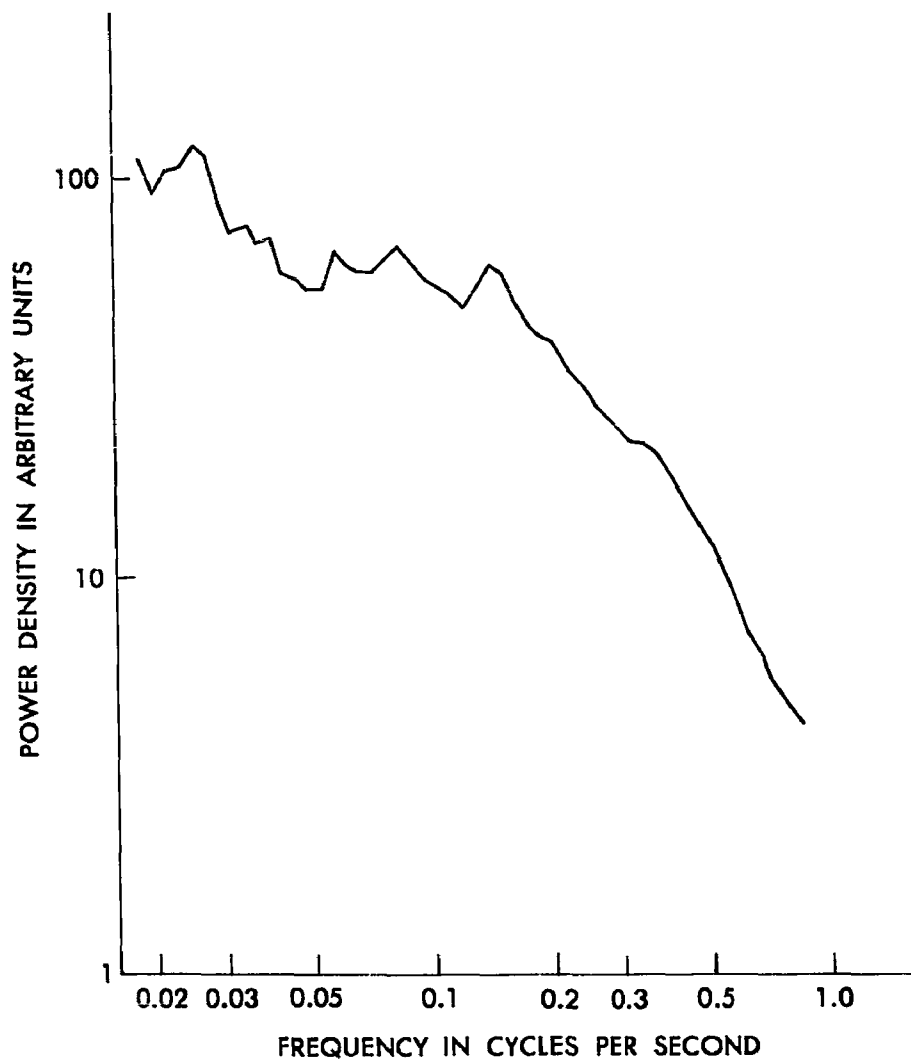


Fig. 10. Power spectral density estimate for the 15.1 mc signal power level fluctuations from 1830:40 to 1848:40 PST on July 31, 1960.

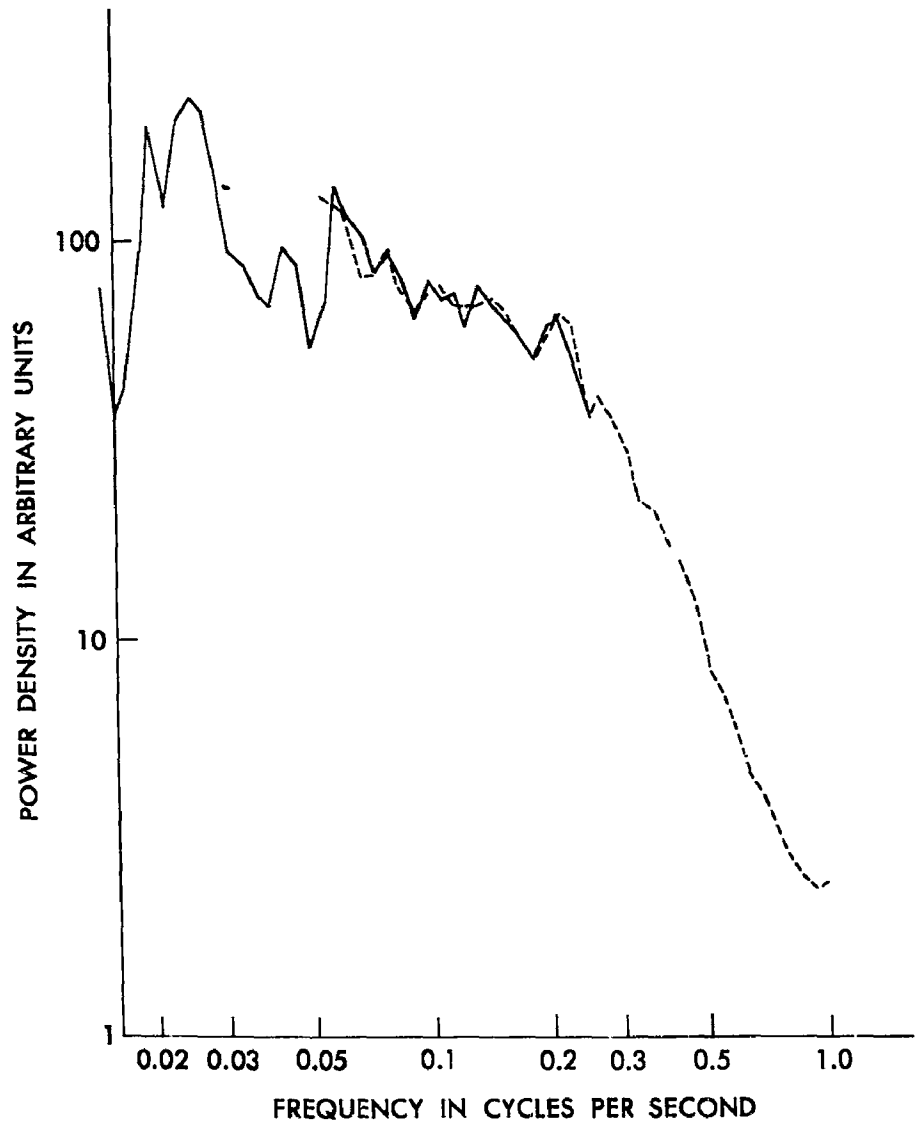


Fig. 11. Power spectral density estimate for the 17.9 mc signal power level fluctuations from 1404 to 1417:30 PST on August 4, 1960. The solid and broken lines represent two separate estimates of the same data.

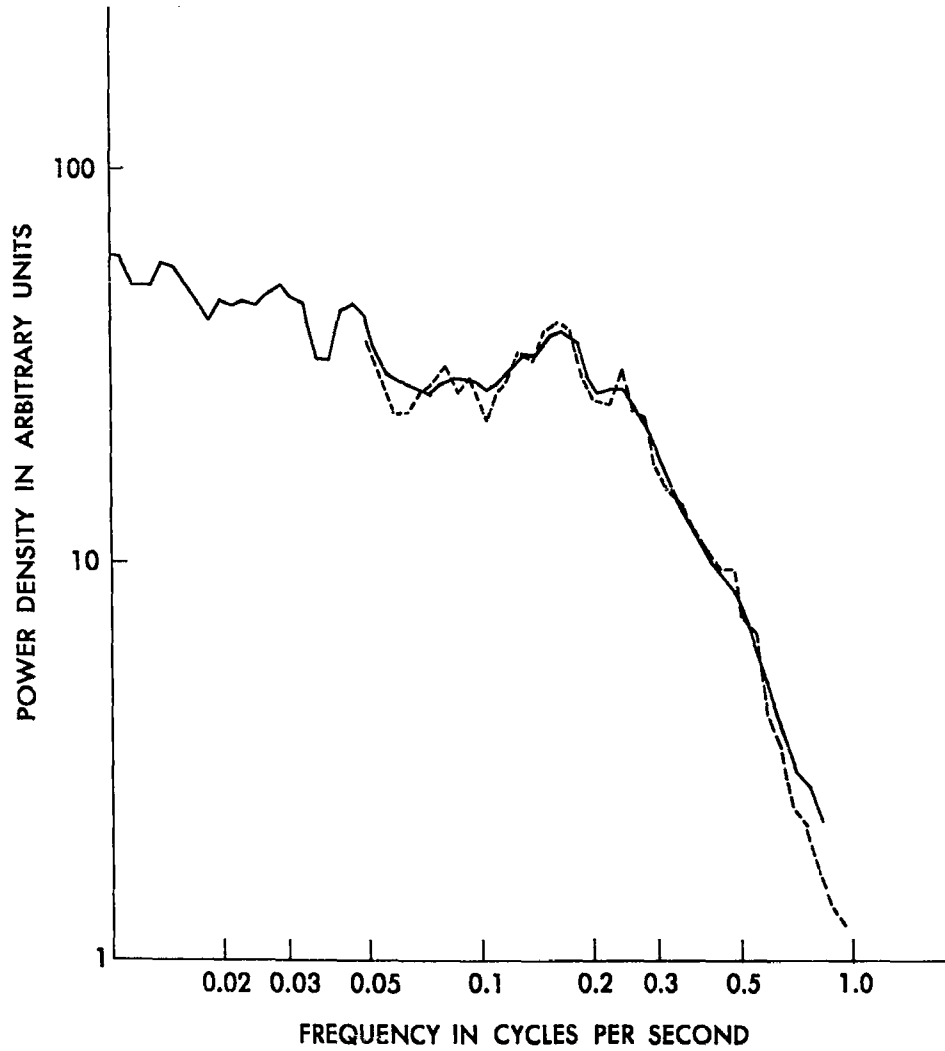


Fig. 12. Power spectral density estimate for the 17.9 mc signal power level fluctuations from 1421 to 1443 PST on August 4, 1960. The solid and broken lines represent two separate estimates of the same data.

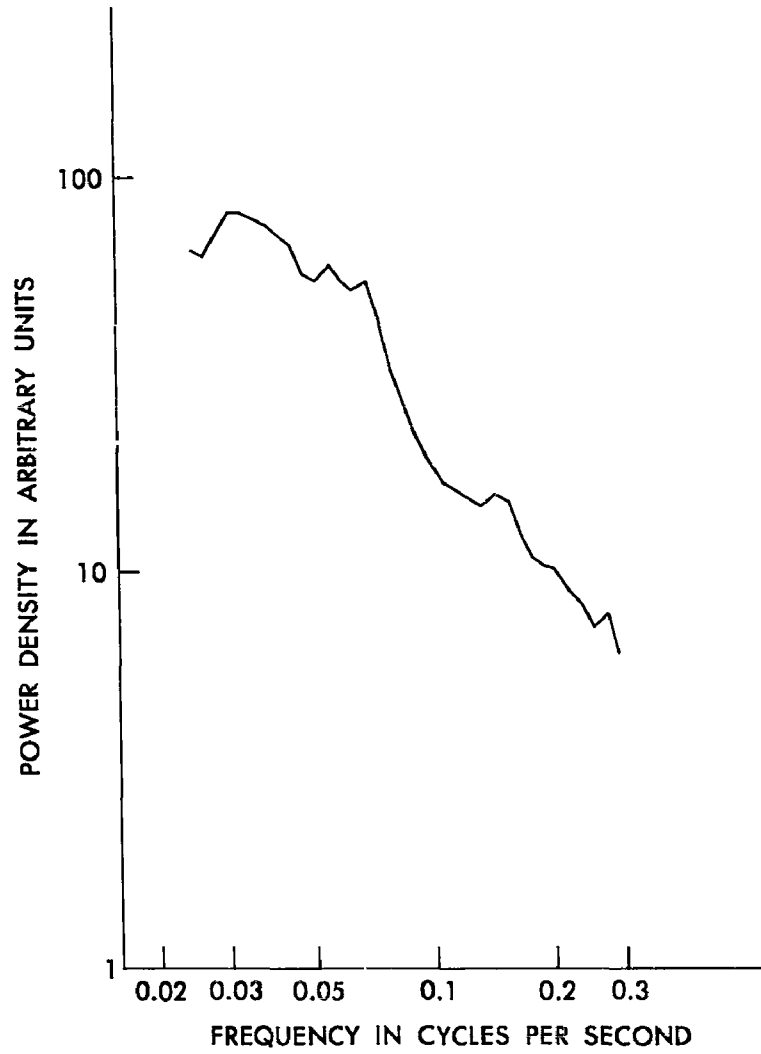


Fig. 13. Power spectral density estimate for the 15.1 mc signal power level fluctuations from 1644 to 1658 PST on September 22, 1960.

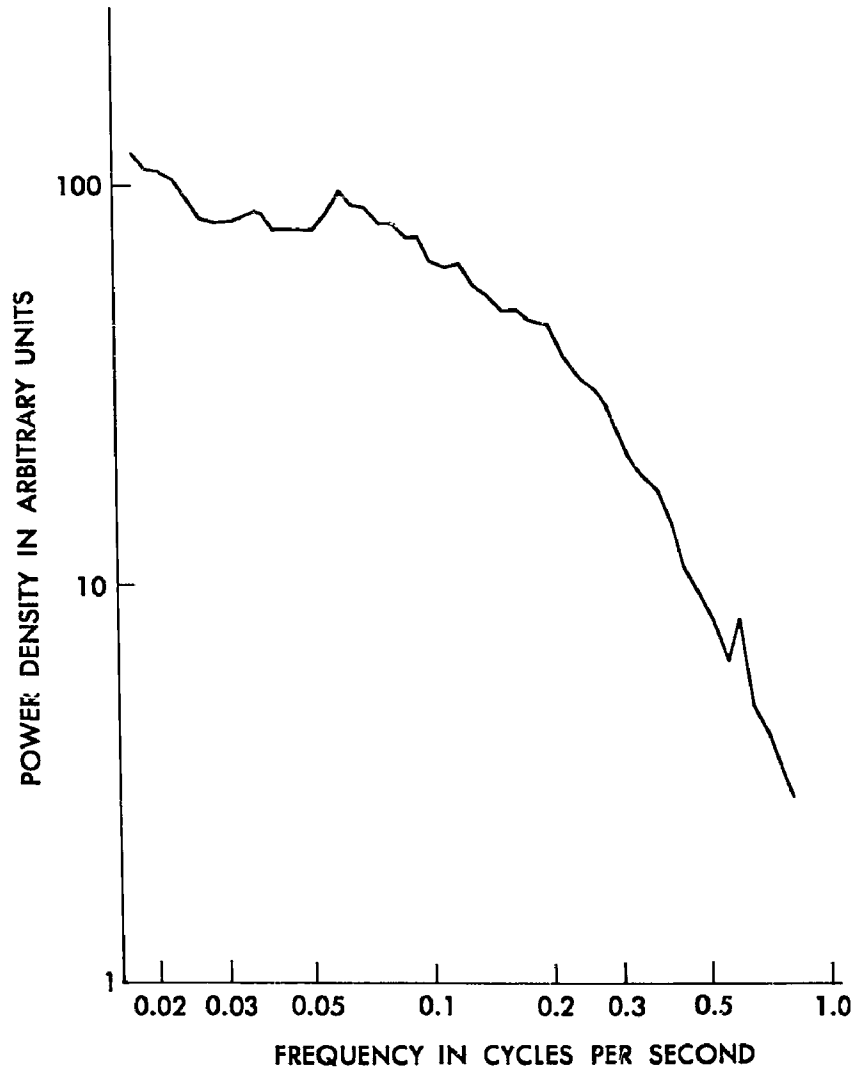


Fig. 14. Power spectral density estimate for the 20 mc WWV signal power level fluctuations from 2249 to 2345 GMT on May 9, 1962.

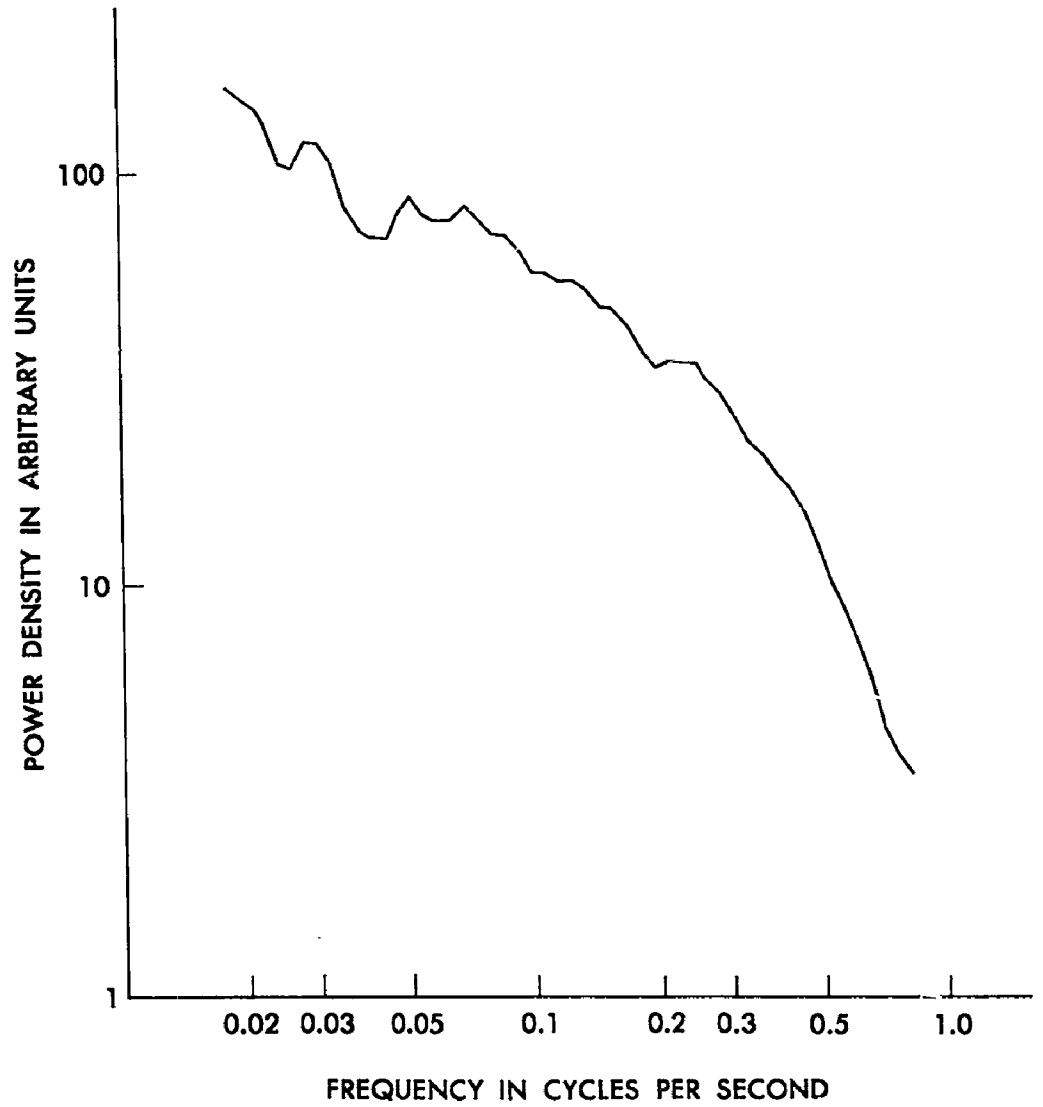


Fig. 15. Power spectral density estimate for the 20 mc WWV signal power level fluctuations from 2349 GMT on May 9, 1962 to 0045 GMT on May 10, 1962.

of a day. However, this is not of prime interest in this study.

The power spectral density estimates for the shorter records are more irregular in shape than those for the 56 minute transmission period of WWV. This is due to the length of the data samples involved, the shorter data samples yielding the less stable estimates.

Two of the graphs, Figures 11 and 12, show two curves each, one solid-line curve and one broken-line curve. These two curves are two separate estimates for the same data. In the case of Figure 11, the two separate estimates were made in order to extend the range of the estimate. In the case of Figure 12, they were made to obtain a measure of the random errors introduced by the computing equipment. This error lies in the neighborhood of three to ten percent as can be seen by comparing the two curves.

The estimate, Figure 13, for the day of September 22, 1960, from 1644 to 1658 PST is likely to be of low validity. The recorded signal was of such small amplitude that the recorder noise level is fairly large with respect to the signal level.

Figures 11 and 12 show two estimates for data samples that are almost consecutive in time. These two estimates

peak at about the same point and have the same general shape except that Figure 11 shows a greater increase in power density at fairly low frequencies.

Figures 14 and 15 also show estimates for data which are consecutive in time. These two estimates drop off to zero at about the same point with about the same rate. Since these two estimates are both for 56 minute long data samples they should be reasonably stable; however, the variance of the estimates is not known.

One interesting facet of the power spectral density estimates is that the frequency range of the fades for the shorter transmission path which entails mostly one or two hops (Figures 14 and 15) is almost identical with the frequency range of the fades for the longer transmission path which entails one, two, three and possibly four hops (Figures 10 through 13). If the fades are due mostly to beating between Doppler-shifted signals arriving via different modes of transmission one might expect a possibly higher frequency range for the greater number of possible hops since the signal will be shifted in frequency at each reflection from a moving ionized layer. These frequency shifts should be cumulative at least part of the time.

Since the quantity of data analyzed is still small the

certainty of any conclusion drawn from the identical frequency ranges is poor.

#### 11. Conclusions

In general, the fading process is a random, quasi-periodic process with a power spectral density falling below one cps. The upper limit of this power density seems to be remarkably constant in frequency.

The most productive method of estimating the power spectral density is with the use of the analog computer. The expected value of the analog computer estimates will converge to the true power spectral density for higher and higher  $Q$  of the simulated resonant circuit. However, the possible spread of the estimates is unknown. It would be desirable to compute the possible spread of the estimate in order to obtain a statistical measure of certainty for the estimates. The mathematical complexity of this computation precluded its inclusion in this report.

APPENDIX A - Equipment

The records of the variation of the amplitude of the incoming wave were in the form of magnetic tape recordings of the diode detector voltage out of a receiver type R-390A/URR, a Collins Radio Company receiver type 51J4, serial number 784, and a Collins Radio Company receiver type 7581, serial number 1524. The rf gain of the receivers was adjusted so that the diode output was proportional to the input.

The magnetic tape recorder used in the experiment was a Precision Instruments model 200 recorder and the tape recordings were made of an FM signal whose frequency deviation was proportional to the amplitude of the signal within plus or minus one percent. The primary data are stored on magnetic tapes.

The tape speeds used for the recording were 7-1/2 inches per second and 0.075 inches per second and the harmonic distortion of the recording system is less than 1-1/2% from 0 to 1250 cps. The original data are in the form of records lasting from fifteen minutes up to an hour. For purposes of computing with these data on the digital computer the original tape was played back through a direct record system and the frequency of the signal was

counted with a Hewlett Packard counter type 522B, and then printed out on paper as a sequence of numbers with a Hewlett Packard type 560A digital recorder. In this fashion the signal was sampled at a maximum rate of one sample every one-tenth of a second. In cases where the variation of the data was small over periods of time that were large with respect to the sample interval time, the time between samples was increased to 1/2 of a second.

Directly counting the frequency of the FM signal on the tape introduces an offset and a scale factor into the original signal by virtue of the fact that zero diode voltage corresponds to 6750 cps. Plus or minus 40% frequency deviation from this depends on d.c. amplifier gain. Consequently the digital computer had to be instructed to convert this set of numbers back to the original data.

Data were also analyzed by using the analog computer as a spectrograph. To speed up this operation we had to change the time scale of the records. This was accomplished by using two tape recorders together and by reproducing the signal at a high tape speed on one machine and re-recording it at a low tape speed on the other machine. The total time reduction obtained by the process was 32 or 64 times depending on the particular set

of data.

The second tape machine used in this process was an Ampex model tape recorder. The shortened recordings obtained with this process were then used in conjunction with a Berkeley Ease analog computer.

The antenna used with the receiver was a three element Yagi antenna mounted approximately sixty feet above the ground. One of the transmission distances involved in the experiment was 6000 km, the transmitter being located in a direction approximately 14 degrees south of east from Seattle.

The transmitter used in part of the experiment was transmitting a cw signal with no modulation except on the hour and half-hour times, during which it was keyed on and off for identification purposes. The other transmitter was WWV in Beltsville, Maryland.

REFERENCES

1. Yeh, K. C., and Villard, O. G., "A New Type of Fading Observable on High-Frequency Radio Transmissions Propagated over Paths Crossing the Magnetic Equator," Proc. IRE, 46, 1968-1970, 1958.
2. Nicholson, P. F., "The Nature of Fading Patterns of Oblique Incidence Radio Signals Received at Middle Latitudes During Certain Ionospheric Disturbances," Research Report, EE 372, School of Elec. Eng., Cornell University, 1958.
3. Wild, J. P., and Roberts, J. A., "The Spectrum of Radio-Star Scintillations and the Nature of Irregularities in the Ionosphere," Jour. of Atmos. and Terr. Phys., 8, 55-75, 1956.
4. Briggs, B. H., and Spencer, M., "Horizontal Movements in the Ionosphere," Reports on Progress in Physics, (Phys. Soc. of London), 17, 245-279, 1954
5. Mitra, S. N., "A Radio Method of Measuring Winds in the Ionosphere," Jour. Inst. Elec. Eng., 96, Part III, 441-446, 1949.
6. Manning, I. A., and Eshleman, V. R., "Meteors in the Ionosphere," Proc. IRE, 47, No. 2, 186-199, 1959.

7. Marmo, F. F., Pressman, J., Manning, E. R., and Aschenbrand, L., "Artificial Electron Clouds V," Planetary and Space Science, 2, 174-186, 1960.
8. Barry, G. H., "Characteristics of Small Scale F-Layer Disturbances Deduced from Narrow Beam Backscatter Soundings," Symposium on the Detection of Ionospheric Perturbations, June 1960.
9. Spencer, M., "The Shape of Irregularities in the Upper Ionosphere," Proc. Phys. Soc., 68-B, Part 8, 493-503, 1955.
10. Court, G. W. G., "Ionospheric Wind Determination from Spaced Radio Receiver Fading Records," Jour. Atmos. Terr. Phys., 7, No. 6, 333-340, 1955.
11. Hoffman, Roger, "Power Spectrum Estimates," Boeing Report Ref. No. JG06, 1960.
12. Blackman, R. B., and Tukey, J. W., "The Measurement of Power Spectra," Dover Pub. Inc., New York, 12, 1958.
13. Bendat, J. S., "Principles and Applications of Random Noise Theory," John Wiley and Sons, 215, 1958.
14. Kendall, M. G., The Advanced Theory of Statistics, 2, Charles Griffin and Company, London, 433, 1948.
15. Grenander, Ulf, and Rosenblatt, Murray, "Statistical Analysis of Stationary Time Series," John Wiley and Sons, New York, 91-94, 1957.

16. Hannan, E. J., "Time Series Analysis," John Wiley and Sons, New York, 52, 1960.

**UNCLASSIFIED**

**UNCLASSIFIED**